Rotational evolution of pre-main sequence stars in Lupus[*]

R. Wichmann[1]**, J. Bouvier**[2]**, S. Allain**[3]**, and J. Krautter**[1]

[1] Landessternwarte Königstuhl, D-69117 Heidelberg, Germany
[2] Canada-France-Hawaii Telescope Corporation P.O. Box 1597 Kamuela, 96743 HI, USA
[3] Laboratoire d'Astrophysique, Observatoire de Grenoble, Université Joseph Fourier, B.P. 53X, F-38041 Grenoble Cedex, France

Abstract. We present results of a study of the rotational periods of Post-T Tauri stars (PTTSs) in the Lupus star forming region. These stars have been discovered by spectroscopic follow-up observations of ROSAT x-ray sources. Photometric observations have allowed to determine their luminosity, and by comparison with theoretical evolutionary tracks they were found to be significantly older on average than typical T Tauri stars.

46 stars have been monitored photometrically, and for 34 of them photometric variations were found that are consistent with rotational brightness modulations caused by starspots. The large number of data on rotational periods of pre-main-sequence (PMS) / zero-age main-sequence (ZAMS) stars available by now allows us to study the impact of stellar mass on the evolution of angular momentum. For several different mass bins, we compare the available data on rotational periods with theoretical models, and find good agreement between theory and observations for the mass-dependency of the pre-main-sequence evolution of angular momentum.

We also study the relation between activity, rotation, mass, and age of low mass stars, and demonstrate that activity is driven by rotation mainly, while it seems to be rather independent of mass and age.

Key words: stars: rotation – stars: pre-main sequence – stars: activity – binaries: eclipsing

1. Introduction

The evolution of stellar surface rotation as a function of age, from the early T Tauri phase through the zero-age main-sequence (ZAMS) up to the age of the present sun, has been one of the central issues in the study of low-mass stellar evolution during recent years.

Observations of the rotation rates of T Tauri stars (TTSs) have shown that TTSs are slow rotators, with rotational periods in the range of $\sim 3 - 10$ days (Bouvier et al. 1993, Edwards et al. 1993, Choi & Herbst 1996). On the other hand, studies of late-type ZAMS dwarfs in young open clusters (Stauffer et al. 1989, Soderblom et al. 1993, Prosser et al. 1995, O'Dell et al. 1995, Allain et al. 1996a, 1996b, 1997) have revealed a large spread of rotation rates among these stars. While in young clusters like α Per up to 50% of the stars are slow rotators with $v \sin i \leq 10$ km/s, there is also a large fraction of ultrafast rotators (UFRs) with projected rotational velocities of up to 200 km/s among the stars investigated. Observations of older clusters (Radick et al. 1987, Soderblom & Mayor 1993) indicate a decrease of the fraction of UFRs as well as of the maximum rotational velocities observed on a timescale of order few 10^8 yrs.

Based on these observations, a picture has begun to emerge which suggests that TTS can be magnetically coupled to their accretion disk, thus forcing them to evolve at more or less constant angular velocity while contracting along the Hayashi track. Only after dissipation of the disk, during evolution toward the ZAMS the star will spin up due to contraction and changes in the internal structure. Finally, during its residence on the main sequence braking by the magnetized stellar wind will spin down the star again.

Within the framework of this picture, in recent years a number of detailed theoretical models have been presented (Bouvier 1994, Bouvier & Forestini 1994, Cameron & Campbell 1993, Cameron & Jianke 1994, Cameron et al. 1995, Keppens et al. 1995). Despite considerable differences in the input physics, all these models can reproduce the general features of the observed evolution of surface rotation reasonably well. For this reason, it it highly desireable to obtain stronger observational constrains on rotational evolution.

In this study we have observed stars with ages between a few 10^6 yrs and about 10^8 yrs, i.e. between the age of the oldest TTSs and the youngest ZAMS cluster dwarfs. According to the models this is the period where the most dramatic changes in the stellar rotation occur, when the internal structure of the star rapidly evolves from a completely convective interior to a

mostly radiative one, and the spin-up occurs that produces the UFRs on the ZAMS.

We briefly present the stellar sample in Sect. 2, and describe the observations and reduction procedures in Sect. 3. The results of these observations are shown in Sect. 4. In Sect. 5.1 we compare our observational data, along with data compiled from the literature, to theoretical model calculations and discuss the implications for the evolution of the angular momentum of pre-main-sequence stars. The relation between stellar activity, rotation, age, and mass is discussed in Sect. 5.2.

2. The stellar sample

In a survey of the Lupus star forming region, follow-up observations of ROSAT x-ray sources by Krautter et al. (1997) lead to the discovery of over 130 hitherto unknown WTTSs, many of them located several degrees outside the Lupus dark clouds. It is not clear as yet, whether these stars have formed in the dark clouds and have dispersed by the small velocity dispersion of a few km/s typically observed in star forming regions (c.f. Jones & Herbig 1979, Dubath et al 1996), as has been suggested by Krautter et al. (1997), or whether they have formed from small cloudlets, as was proposed by Feigelson (1996). However, both explanations require that at least a large fraction of these newly discovered, 'dispersed' WTTSs are significantly older (i.e. some 10^7 yrs old) than the TTSs found near the dark clouds in star forming regions.

Based on a numerical model of X-ray sources near the galactic plane, Briceño et al. (1997) suggested that the 'dispersed' ROSAT WTTSs are not at all related to the SFRs where they have been discovered. They suppose that these stars are members of a foreground population of spatially homogeneously distributed galactic ZAMS stars completely unrelated to SFRs. However, this idea is ruled out by the results of a recent study of the spatial distribution of 'dispersed' WTTSs near Lupus by Wichmann et al. (1997b). This study shows that the spatial distribution of these stars is correlated with the Gould Belt (i.e. they are most probably members of the Gould Belt, like the Lupus SFR), while no WTTSs could be found in the galactic plane, contrary to the predictions of the model by Briceño et al. (1997). This contradiction is not unexpected, as the Briceño et al. model does not take into account the overdensity of young, X-ray active stars in and near SFRs.

A thorough study of the 'dispersed' WTTSs discovered by Krautter et al. (1997) has been performed by Wichmann et al. (1997a). Using bolometric luminosities determined from BVRI photometry and effective temperatures estimated from spectral type, they could place a large fraction of these stars in the HR diagram and determine ages and masses by comparison with theoretical evolutionary tracks (D'Antona & Mazzitelli 1994). Their results show that indeed these 'dispersed' WTTSs on average have ages of a few 10^7 yrs, significantly in excess of the typical age of several 10^6 yrs found for the Lupus TTSs near the dark clouds (Hughes et al. 1994).

This age estimate for the Lupus 'dispersed' WTTSs is in line with their membership to the Gould Belt. The Gould Belt

is a young, expanding structure with an age of some $5 - 6 \times 10^7$ yrs (c.f. Comerón et al. 1994, Westin 1985). Note that the Lupus SFR is located not inside the Gould Belt, but rather at the periphery of this structure, opposite to its center as seen from the Sun (which is located about halfway between both). Presumably it has formed at some time after the expansion of the Gould Belt has started, i.e. it is younger than the Gould Belt as a whole.

Thus, many of the WTTSs found by Krautter et al. (1997) apparently populate a range of ages which is intermediate between that of typical TTSs and that of ZAMS clusters. We therefore regard these objects as 'Post-T Tauri stars' (PTTSs), following Herbig (1978) who was the first to predict the existence of this population of PMS stars. We will henceforth use this term to denote the stars of our sample. We also apply this term to the stars studied by Bouvier et al. (1997a) in a campaign similar to this work, but aimed at PTTSs discovered by Wichmann et al. (1996) in the Taurus-Auriga star forming region.

On theoretical grounds, Palla & Galli (1997) have concluded that such a population of PTTSs in or near a SFR might not be expected. They argue that the timescale of ambipolar diffusion is comparable to the lifetime of molecular clouds. Thus star formation would be inhibited for most of the lifetime of the cloud, and the resulting range of stellar ages would be quite narrow. However, while large molecular clouds containing OB associations might be disrupted by stellar winds and supernova explosion on short timescales, the lifetimes of smaller clouds harbouring T Tauri associations are quite uncertain, but might be much larger (c.f. Elmegreen 1985). Thus there seems to be no compelling reason to apply the conclusions of Palla & Galli (1997) to low-mass SFRs.

Based on the results of Wichmann et al. (1997a), we have selected from the sample of Krautter et al. (1997) stars covering some range of masses ($\sim 0.4 - 1.1 M_\odot$) and ages (a few 10^6 to a few 10^7 yr), in order to study the dependency of rotation on these parameters.

3. Observations

A sample of 46 PTTSs in Lupus has been observed in two observing runs at the 0.9 m Dutch telescope at ESO, La Silla, in order to derive rotational periods from brightness modulations caused by starspots. The two runs took place from May 4, 1995 to May 19, 1995, and from May 1, 1996 to May 10, 1996. In both runs we used the CCD camera with the TEK # 33 and Johnson B and V filters. However, due to unfavourable weather, for the first run the sampling in the B band is significantly worse than in the V band. As we intended only differential photometry, no photometric standard stars were observed. Twilight flatfield images were obtained following the prescription of Tyson & Gal (1993), which was found to be very helpful.

Data reduction was performed at Landessternwarte Heidelberg using the IRAF 'ccdred' and 'phot' packages. After debiasing and flatfielding, the magnitudes of the target star and of several comparison stars were determined on each image of the target star. Then, after rejection of possibly variable comparison
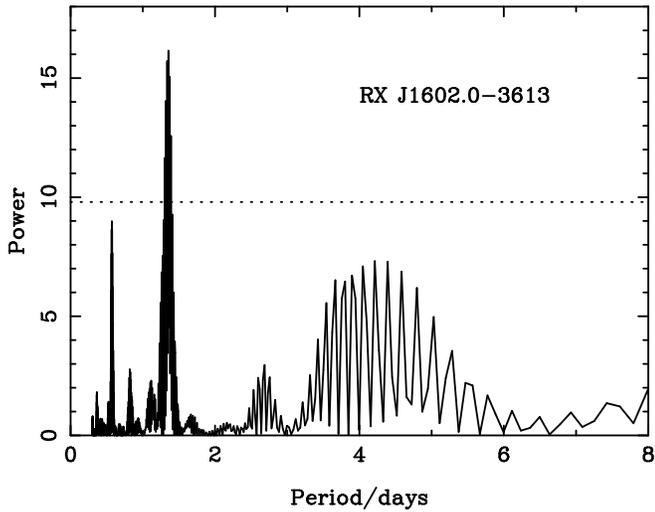
Fig. 1. Periodogram of RX J1602.0-3613. Dashed line shows the 0.999 significance level.

Fig. 2. Histogram of periods found for Lupus PTTSs.

stars, the mean instrumental lightcurve of the comparison stars was computed and subtracted from the instrumental lightcurve of the target star. This procedure was applied independently to both the V band and B band images of each target star. Typically about four to six comparison stars were used for each target star, and the resulting (1σ) overall error was found to be about 0.01 mag on average.

4. Results

4.1. Period determination

Three different algorithms were employed to search for periods: (1) the periodogram analysis (Scargle 1982, Horne & Baliunas 1986),(2) the CLEAN algorithm (Roberts & Dreher 1986) and (3) the string-length method introduced by Dworetzky (1983). The statistical significance of the result of the periodogram analysis was established by computing false-alarm probabilities using a Monte-Carlo method as described in Bouvier et al. (1993). A sample periodogram from the Scargle algorithm is shown in Fig. 1. Amplitudes were estimated by least-square fitting of a function of the form $a\sin{(T/2\pi P)} + b\cos{(T/2\pi P)}$, where P denotes the period as determined from the periodogram analysis, T the time, and a and b free parameters. (Photometric variations due to surface spots are not necessarily sinusoidal, and fitting a pure sine function often produced poor results only.)

In Table 1 we present results for all stars for which the statistical significance of the period derived by the periodogramm analysis exceeds 0.999 (34 out of a total of 46 observed stars). We also list ages and masses as derived by Wichmann et al. (1997a), the x-ray luminosity L_X as given in Krautter et al. (1997), and $\log L_X/L_{bol}$, the ratio of x-ray luminosity to bolometric luminosity L_{bol}, which frequently is used to parametrize the coronal activity of a star. The phased lightcurves for these stars are shown in Fig. 3.
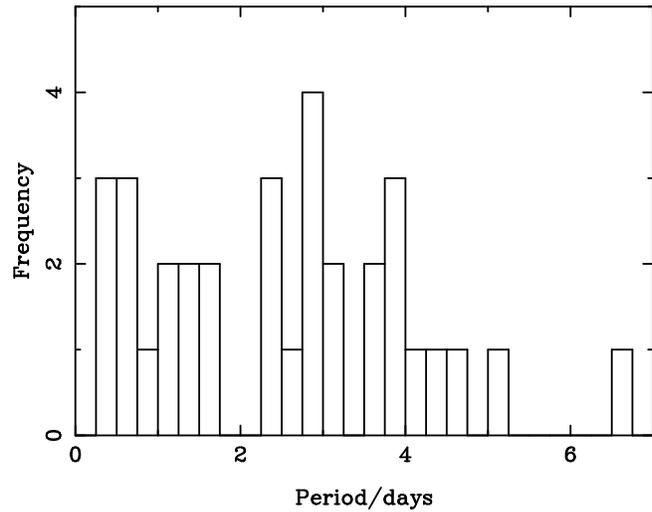
A histogram of the observed periods for Lupus PTTSs is shown in Fig. 2. Almost all stars are found in the range of 0.25–5 days, while only four stars (including two lower limits) with longer periods were found. This is in strong contrast to the distribution of periods as found for WTTS (c.f. Bouvier 1993), where about half of the stars have periods longer than five days. Thus we see a strong evolution of angular velocity from TTSs to PTTSs, a conclusion also reached by Bouvier et al. (1997a) in their study of Taurus PTTSs.

Only three stars were observed in both runs: RXJ1517.8-3706A/B and RXJ1525.6-3537. For RXJ1517.8-3706B, the same period was found in both runs. For RXJ1517.8-3706A, no period could be found in the first run. This might be due to the absence of any large spot on the star during the first. However, the lower data quality (due to the weather conditions), in combination with the low amplitude of the variations, does not allow us to draw any firm conclusions. For RXJ1525.6-3537, in both runs the best period is very close to 1d. Unfortunately, the phase shift between both runs seems to be also close to a multiple of one day, as the phased lightcurve of the combined data still spans only half the phase.

4.2. Selection effects

We consider four possible selection effects which might affect the actually observed distribution of periods. First, the amplitude of the photometric variability might depend on the period. In order to study this, we have compiled from the literature data on TTSs (Bouvier et al. 1993, Choi & Herbst 1996, the compilation by Neuhäuser et al. 1995 and references therein), PTTSs (Bouvier et al. 1997a) and ZAMS clusters (Stauffer et al. 1989, Soderblom et al. 1993, Prosser et al. 1995, O'Dell et al. 1995, Allain et al. 1996a). In Fig. 4, we plot the photometric amplitude ΔV vs. the rotational period P for CTTSs, WTTSs/PTTSs and ZAMS stars (due to the restriction to stars with both ΔV and P published, the typical bimodal distribution
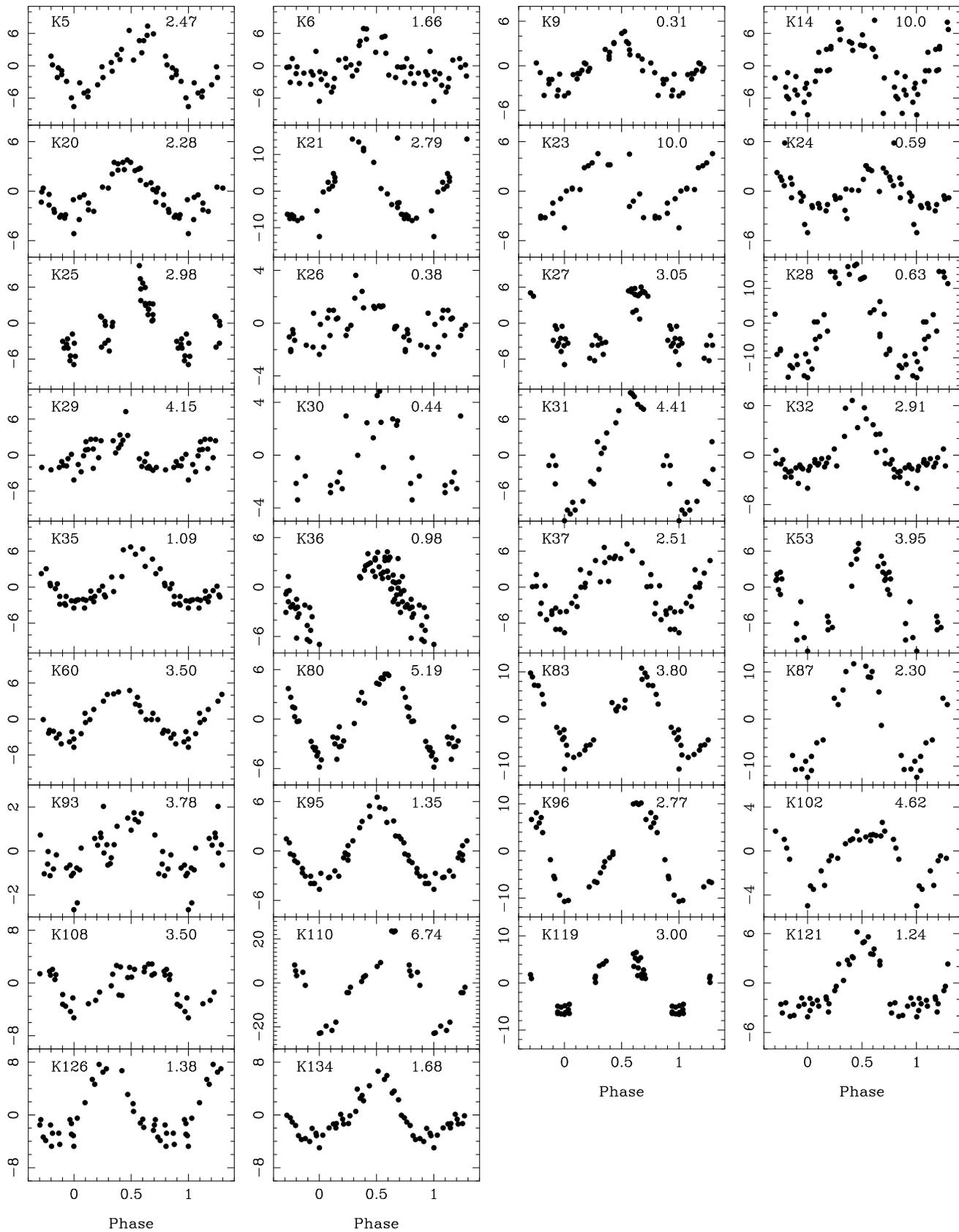
Fig. 3. Phased V-band lightcurves for Lupus PTTSs. The differential magnitude is given in 10^{-2} mag. For each star, in the upper left corner the name, in the upper right corner the period (in days) is noted.

Table 1. Data on Lupus PTTSs for which rotational periods could be measured in this work. We list (1) the number of the star in the Krautter et al (1997) survey, (2) Designation, (3) Right ascension, (4) Declination, (5) period P, and amplitudes (6) ΔV and (7) ΔB in the V and B bands, respectively. In addition, we give (8) ages and (9) masses as derived by Wichmann et al. (1997b), the X-ray luminosity (10) $\log L_X$ as given in Krautter et al (1997), and (11) $\log (L_X/L_{bol})$, the ratio of X-ray luminosity to bolometric luminosity (where the latter is taken from Wichmann et al. (1997a)). For ΔV of K93 and ΔB of K108 no good fits could be obtained. [U]Periods for K14 and K23 are lower limits only.

K	Designation	RA (2000.0)	Dec (2000.0)	P [days]	ΔV [mag]	ΔB [mag]	Log(age) [yrs]	Mass [$M_\odot$]	$\log L_X$ [erg/sec]	$\log (L_X/L_{bol})$
5	J1507.6-4603	15:07:37.6	-46:03:14	2.47	0.05	0.05	7.11	1.04	30.08	-3.28
6	J1507.9-4515	15:07:54.4	-45:15:21	1.66	0.03	0.04	7.37	1.05	30.05	-3.58
9	J1508.6-4423	15:08:37.6	-44:23:16	0.31	0.03	0.03	7.15	1.13	30.55	-3.02
14	J1514.0-4629A	15:14:01.0	-46:29:42	10.00[U]	0.06	0.07	6.57	0.29	29.83	-2.79
20	J1515.8-3331	15:15:45.3	-33:31:59	2.28	0.03	0.04	6.93	1.28	30.33	-3.37
21	J1515.9-4418	15:15:52.8	-44:18:16	2.79	0.10	0.11	7.43	0.88	30.36	-2.86
23	J1517.8-3706A	15:17:50.1	-37:06:41	10.00[U]	0.03	0.03	7.11	0.34	29.89	-2.45
24	J1517.8-3706B	15:17:50.1	-37:06:41	0.59	0.04	0.03	6.61	0.61	29.94	-3.09
25	J1518.5-3738	15:18:26.8	-37:38:02	2.98	0.05	0.06	6.87	1.22	30.49	-3.09
26	J1518.9-4050	15:18:52.8	-40:50:52	0.38	0.02	0.02	7.03	1.23	30.07	-3.60
27	J1519.3-4056	15:19:16.0	-40:56:07	3.05	0.05	0.06	7.09	1.15	30.70	-2.87
28	J1522.2-3959	15:22:11.7	-39:59:50	0.63	0.15	0.16	6.97	1.04	30.44	-2.89
29	J1523.4-4055	15:23:25.5	-40:55:46	4.15	0.02	0.03	7.17	1.01	30.04	-3.30
30	J1523.5-3821	15:23:30.5	-38:21:18	0.44	0.05	0.05	6.27	0.30	29.92	-2.92
31	J1524.0-3209	15:24:03.1	-32:09:49	4.41	0.10	0.10	6.25	0.65	30.23	-3.13
32	J1524.5-3652	15:24:32.4	-36:52:03	2.91	0.03	0.02	7.09	1.08	30.19	-3.24
35	J1525.5-3613	15:25:33.1	-36:13:47	1.09	0.04	0.04	6.93	1.14	30.44	-3.04
36	J1525.6-3537	15:25:36.7	-35:37:32	0.98	0.06	0.07	6.53	0.80	30.60	-2.71
37	J1526.0-4501	15:25:59.7	-45:01:15	2.51	0.05	0.05	7.31	1.05	30.25	-3.35
53	J1538.0-3807	15:38:02.6	-38:07:23	3.95	0.08	0.07	7.01	0.92	30.22	-2.94
60	J1540.7-3756	15:40:41.2	-37:56:18	3.50	0.04	0.03	6.81	0.86	30.08	-3.09
80	J1550.0-3629	15:49:59.0	-36:29:57	5.19	0.05	0.05	7.03	1.08	30.00	-3.41
83	J1552.3-3819	15:52:19.4	-38:19:31	3.80	0.08	0.08	7.17	0.81	29.44	-3.51
87	J1555.6-3709	15:55:33.8	-37:09:40	2.30	0.11	0.12	6.83	0.86	29.84	-3.32
93	J1601.2-3320	16:01:08.9	-33:20:14	3.78	-	0.01	6.93	1.32	30.17	-3.57
95	J1602.0-3613	16:01:59.0	-36:12:55	1.35	0.05	0.05	6.77	1.09	30.44	-3.01
96	J1603.2-3239	16:03:11.7	-32:39:20	2.77	0.11	0.11	6.85	0.81	30.22	-2.88
102	J1605.6-3837	16:05:33.3	-38:37:43	4.62	0.03	0.04	6.83	0.41	29.97	-2.69
108	J1608.3-3843	16:08:18.2	-38:44:05	3.50	0.03	-	6.33	0.68	30.46	-2.88
110	J1608.5-3900A	16:08:28.4	-39:00:30	6.74	0.19	0.17	6.55	0.35	29.96	-2.78
119	J1609.7-3854	16:09:39.6	-38:55:07	3.00	0.06	0.07	5.97	0.73	30.04	-3.66
121	J1610.1-4016	16:10:04.8	-40:16:12	1.24	0.04	0.04	6.87	1.17	30.46	-3.06
106	J1613.0-4004	16:13:02.4	-40:04:22	1.38	0.05	0.07	6.37	0.69	29.65	-3.65
134	HD 147402	16:23:29.5	-39:58:01	1.68	0.04	0.05	7.41	1.03	30.36	-3.22

of WTTS/CTTS might not be apparent in this diagram). There is indeed an obvious trend for the stars with the longest periods also to show the largest amplitudes. However, these large amplitudes are observed only for CTTSs, i.e. stars still accreting material from their circumstellar disks. As discussed by Bouvier et al. (1993), the variability of these stars is caused by *hot* spots resulting from the accretion process, contrary to the *cool* solar-like spots observed in non-accreting stars like WTTSs, PTTSs and ZAMS stars. Similar conclusions have been reached by Vrba et al. (1993). If we take into account only the latter, i.e. stars with cool spots, no dependency of amplitudes on periods is discernible within this range of rotational periods. Note how-

ever, that O'Dell et al. (1995) find very low amplitudes for very slowly rotating (main-sequence) stars ($P \gtrsim 30d$).

Second, in their study of ZAMS stars, Allain et al. (1996b) could find periodic variations for 7/10 (7 out of 10) K stars, but only for 3/11 G stars. They conclude that, within their sample, amplitudes might depend on spectral type (i.e. depth of convective zone). We find mean amplitudes $\Delta V = 0.03 \pm 0.01$, 0.06 ± 0.03, and 0.06 ± 0.06 for G, K, and M stars, respectively (spectral types are taken from Krautter et al. 1997). According to Student's t-test, the probability of ΔV being equal for both G and K stars is 0.014. Thus our results support the conclusion of Allain et al. (1996b). However, we detect periodic variations for 6/7 G stars, 21/26 K stars and 6/12 M stars (the remaining star
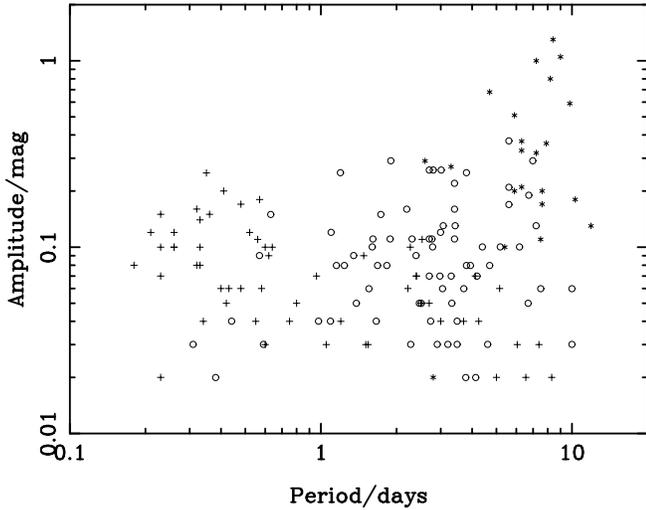
Fig. 4. Photometric amplitude in the V band vs. rotational period for CTTSs (stars), WTTSs/PTTSs (circles), and ZAMS stars(crosses).
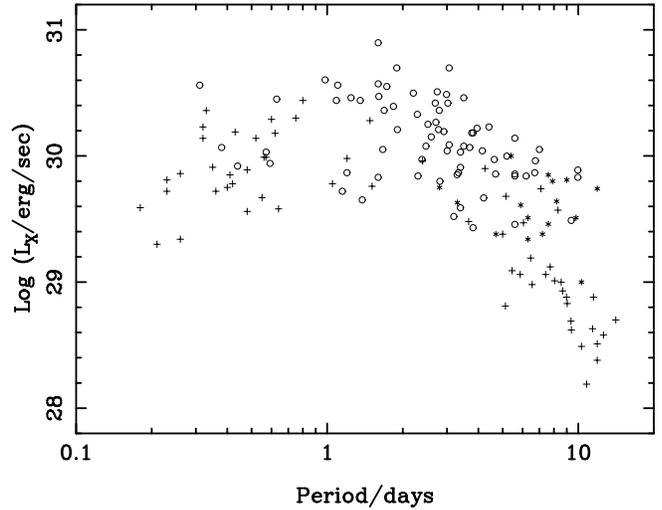
Fig. 5. X-ray luminosity L_X vs. rotational period for PMS/ZAMS stars. Symbols as in Fig. 4.

is an eclipsing binary). Thus the lower photometric amplitude in stars of earlier spectral type seems negligible with respect to the results of our study.

Third, as the survey of Krautter et al. (1997) was based on x-ray data, a correlation of x-ray luminosity with stellar rotation would also introduce a bias in our observed period distribution. In Fig. 5, we have combined x-ray data for TTSs from Neuhäuser et al. (1995), for PTTSs from Wichmann et al. (1997a) and Krautter et al. (1997), for α Per from Randich et al. (1996), for Pleiades from Stauffer et al. (1994) and for Hyades from Stern et al. (1995) and Pye et al. (1994). (Note that these data should not be regarded as representing the typical x-ray luminosities of the respective samples, as there is a selection effect due to the flux-limited x-ray observations.) Obviously, some dependency of log L_X on rotational period is present. In particular, the very slow rotators tend to show very low x-ray luminosities. Thus most probably the x-ray-selected samples of PTTSs are biased towards rapid rotators. This implies that we will not be able to learn about the origin of the slow rotators on the ZAMS, a conclusion also reached by Bouvier et al. (1997a) in their investigation of Taurus-Auriga PTTSs. Apparently our sample is more useful to study the lower envelope of the evolution of rotational periods, i.e. the upper envelope for angular velocities. (The relation between x-ray activity and rotation will be discussed in more detail in Sect. 5.2).

Finally, also the sampling of our photometric observations could introduce some bias. We have observed with a sampling frequency of 3-4 observations/night for a period of 16 (first run) or 10 (second run) days, thus a *conservative* estimate of the range of discernible periods would be 0.3-10 days (if we would take into account the non-regularity of the sampling, the lower limit would be even smaller). Moreover, as the amplitude of variations seems not to depend on the period, we should also be able at least to detect clear variability for stars out of this range that have large spots. There are in fact two stars with marked short-term

photometric variability for which no period could be determined (RXJ1556.1-3655 & RXJ 1608.5-3847). However, RXJ1556.1-3655 is a CTTS with about 70Å equivalent width in the Hα-line, and RXJ 1608.5-3847 is a borderline case (EW(Hα) $\approx$ 7Å). As disk-accreting CTTS often show irregular variability (c.f. Appenzeller & Mundt 1989, Gahm et al. 1989), we regard the latter as the more likely explanation for the non-detection of periodicity. At the upper limit, two objects are discovered with periods of $\gtrsim$ 10 days.

Thus we conclude that with respect to the observed distribution of periods, the only strong selection effect within our sample is a bias against the detection of long periods, which is due to the x-ray selection of the sample.

4.3. RXJ1608.6-3922

In the course of our observations, RXJ1608.6-3922 was identified as eclipsing binary with an orbital period of about 7.2 days. The V lightcurve of the star is displayed in Fig. 6. From the orbital period as well as from the small difference in luminosity between the two components, we expect this object to be a double-lined spectroscopic binary. Thus this object might be useful for the determination of the masses of the individual components.

5. Discussion

5.1. Rotational evolution

The main subject of our study has been the investigation of the evolution of surface rotation during the PMS phase and its mass-dependency. For this purpose, photometrically derived rotational periods have significant advantages over projected rotational velocities as measured from high-resolution spectra, not only because they are free of the uncertainty introduced by the projection factor sin i, but also because they directly yield the
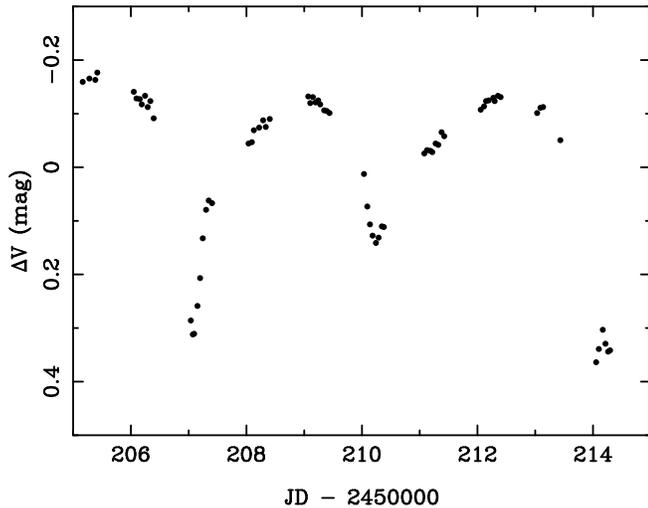
Fig. 6. Instrumental lightcurve in the V band for the eclipsing binary RXJ1608.6-3922.

angular velocity $\Omega = 2\pi/P$, which is the prime physical parameter involved in the theoretical modelling of the rotational evolution.

Except for the very recent work of Bouvier et al. (1997a) on Taurus PTTSs, previous studies of rotational evolution have concentrated either on young PMS stars, or on stars on the ZAMS or beyond. The present study therefore yields an important contribution to fill the observational gap between TTSs and ZAMS.

To cover the full range of PMS/ZAMS evolution, we have supplied our data with data from the literature as mentioned in Sect. 4.2. For the Orion stars of Choi & Herbst (1996), luminosities were calculated using the photometry given in Edwards et al. (1993), and a bolometric correction in the I band (Bessel & Wood 1984). Ages then were estimated using the set of D'Antona & Mazzitelli (1994) evolutionary tracks calculated with Canuto–Mazzitelli convection theory (Canuto & Mazzitelli 1991) and opacities from Alexander et al. (1991). For the open cluster stars, B-V has been converted to masses using main-sequence relations. This is an approximation only, but errors are small compared to the size of the mass bins we use.

The resulting dataset is illustrated in Fig. 7, where we plot periods vs. stellar age for three different mass bins: $0.4-0.7M_\odot$, $0.7-0.9M_\odot$ and $0.9-1.2M_\odot$. (This particular choice of mass bins is mainly dictated by the available dataset and the aim to have the diagrams not too sparsely populated.) For all three mass bins, we clearly see the spin-up in the PMS phase which is now widely believed to result from contraction and structural changes in the star during the PMS evolution, leading to a decrease of the moment of inertia. Also apparent is the spin-down at later times which is due to braking by the magnetized stellar wind. Note that slow ZAMS rotators are under-represented in the plots due to lack of data.

In comparing the three mass bins, it seems that towards lower masses the shortest observed periods occur at higher stellar ages.

For the highest masses $(0.9 - 1.2M_\odot)$ we find PTTSs with rotational periods as short as in the α Per ZAMS clusters. In the next lower mass bin $(0.7 - 0.9M_\odot)$, the α Per stars show the shortest rotational periods. Finally, in the lowest mass bin $(0.4 - 0.7M_\odot)$, the PTTSs seem to be still in the spin-up phase, as their shortest rotational periods are well above that of the α Per and Pleiades stars. However, we also see that stars of all masses reach very short rotational periods on the order of a few hours, corresponding to velocities of $150 - 200$ km/sec.

A two-sample K-S test shows that the difference in period distribution between the low-mass and the high-mass subsample of PTTSs is significant at the 8 per cent level (probability for equal parent populations). However, this might be an upper limit only for the similarity of both samples. The reason is that both subsamples are biased towards rapid rotators, as discussed above, and that the low-mass subsample, due to the intrinsic faintness of the stars, probably is less complete than the high-mass subsample. A statistical comparison would only be meaningful if both (sub)samples were either random or would represent the same fraction of the tail of rapid rotators in the parent population.

A shift of the period distribution is expected as a consequence of the longer contraction timescale towards the ZAMS for lower masses, which causes the moment of inertia to decrease much slower. As a result, already during the spin-up phase the braking by the magnetized stellar wind will play an important role for lower masses, contrary to higher masses, where the spin-up timescale is much shorter than the braking timescale. If, in theoretical models, the same braking law is used for all masses, stars with low masses would inevitably not spin up as much as stars with high masses, contrary to observations. This means that in theoretical models the braking law has to be mass-dependent, i.e. it has to be weaker for lower mass stars.

Following this idea, a set of theoretical tracks for the evolution of surface rotation with a mass-dependent braking law has been calculated recently by Bouvier et al. (1997b). In this model the mass-dependency is introduced by merely changing the velocity above which the transition from $d\Omega/dt \propto -\Omega^3$ to $d\Omega/dt \propto -\Omega$ occurs (where Ω denotes the angular velocity). The transition in the braking law occurs at $14\,\Omega_\odot$ for $1\,M_\odot$ stars, $8\,\Omega_\odot$ for $0.8\,M_\odot$ stars, and at $3\,\Omega_\odot$ for $0.5\,M_\odot$ stars (see Bouvier et al. 1997b for more details).

In Fig. 7, we have overplotted these tracks on our data. There is very good agreement between data and model for the $0.7 - 0.9M_\odot$ bin, and also for the $0.9 - 1.2M_\odot$. Only few stars are seen with slightly shorter rotational periods than predicted by the lower tracks. However, while all these tracks are computed for a unique initial period of 8 days, in reality there will be some scatter in the initial period distribution. A few stars will start with shorter periods in the range $4 - 8$ days, and these may account for the few PMS stars which lie slightly below the lower track.

For the lowest mass bin, there is somewhat less agreement between data and model. The observed shift of the peak of the period distribution is reproduced by the model. However, for the low mass bin the peak in the model tracks seems to occur later than in the observed data. Within the model the peak, which
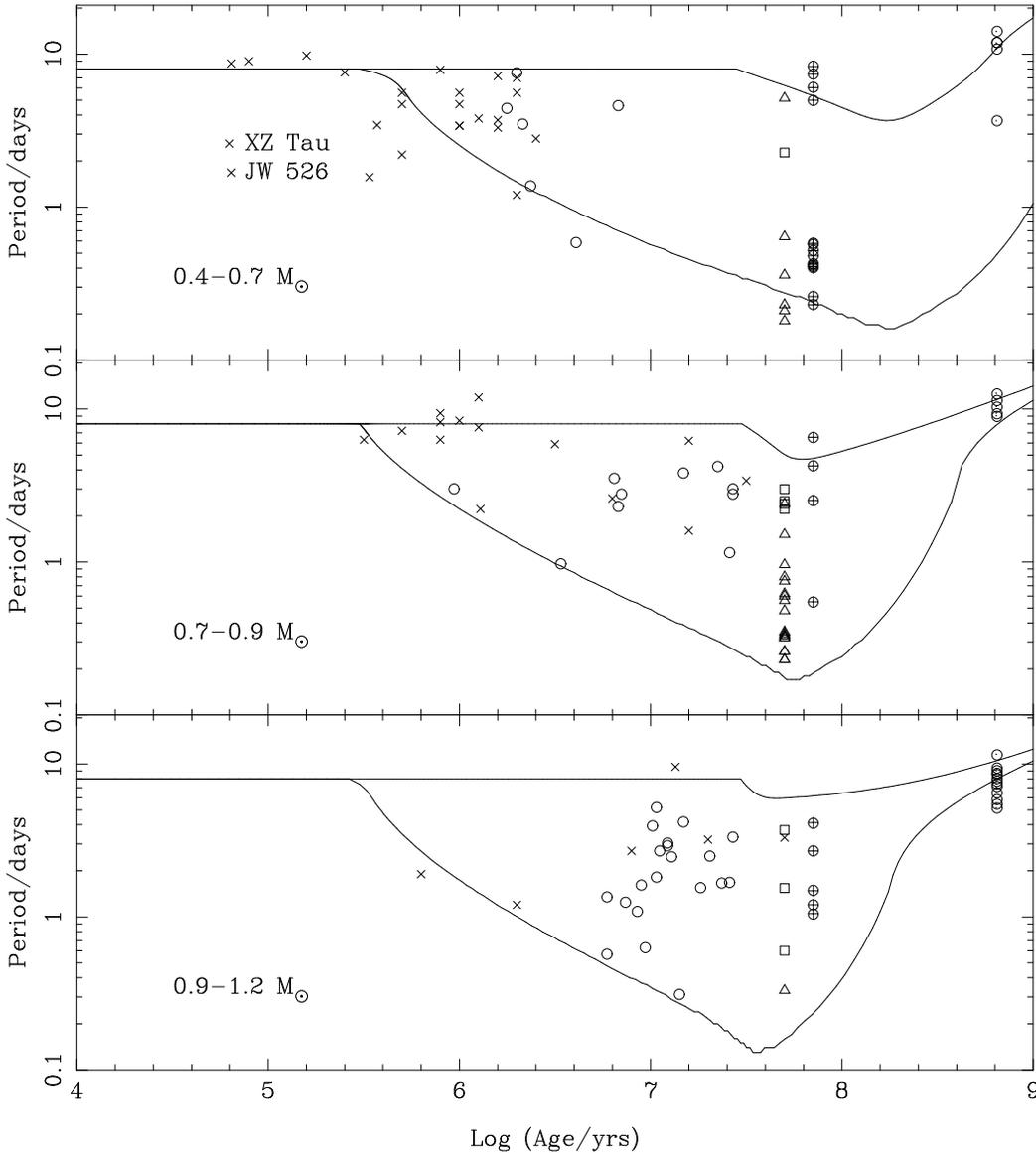
Fig. 7. Rotational periods vs. stellar age for different samples of PMS/ZAMS stars in three mass bins. From top to bottom: $0.4M_\odot \leq M \leq 0.7M_\odot$, $0.7M_\odot < M \leq 0.9M_\odot$, $0.9M_\odot < M \leq 1.2M_\odot$. Crosses: TTSs, circles: PTTSs, triangles: α Per, boxes: IC 4665, encircled crosses: Pleiades, and encircled dots: Hyades. For each mass bin, we plot two theoretical tracks from Bouvier et al. (1997) for $0.5M_\odot$, $0.8M_\odot$, and $1.0M_\odot$, respectively. In each mass bin, the two tracks are calculated for disk lifetimes of 3×10^7 yrs (upper track) and 3×10^5 yrs (lower track).

is mainly determined by the long contraction timescale for low masses, can only be shifted towards an earlier age if the braking is increased, but then the Hyades would not be fitted. On the other hand, taking again into account some dispersion in the initial periods, nearly all of the α Per and Pleiades stars lie above the lower rotational evolution track if we start with an initial period of $P = 4$ days. Whether the peak in the model really occurs too late is then difficult to say since we would need data for a 200 Myr cluster to answer this question.

Very interesting, however, are the two very young low mass stars with rather short periods that appear in this plot. One is XZ Tau, for which Simon et al. (1993) give an age of 7×10^5 yrs.

The star is a binary, and Simon et al. take into account the flux ratio of the separate components to calculate the luminosity, thus the argument that the star would shift to an higher age, if binarity is taken into account, seems *not* valid here. Bouvier et al. (1993) report a period of 2.6 days, albeit only at the 90% confidence level, and discuss the possibility that this is the orbital period of a spectroscopic binary. However, they conclude that a hot spot on the star is a more likely explanation.

The other star is JW526, for which Choi & Herbst (1996) report a period of 1.69 days at a very high confidence level ($> 99\%$). We have estimated its age to 6×10^5 yrs in the way mentioned above. Edwards et al. (1993) have shown that the
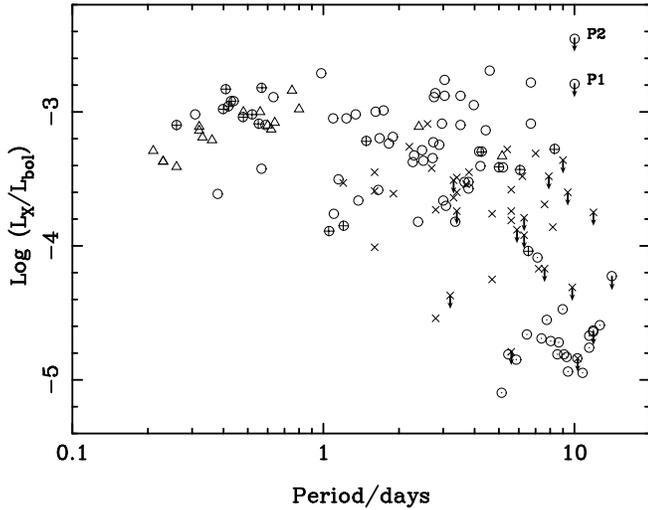
Fig. 8. Log (L_X/L_{bol}) vs. rotational period for different samples of PMS/ZAMS stars. Different samples are denoted by the same symbols as in Fig. 7
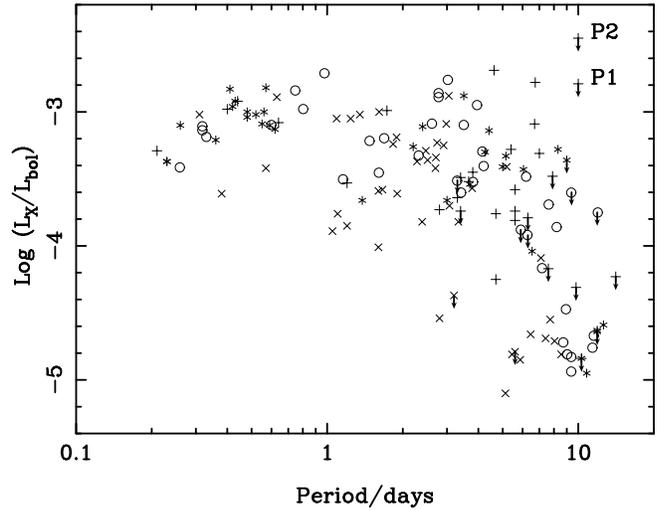
Fig. 9. Log (L_X/L_{bol}) vs. rotational period for the quartiles of the mass distribution of the data set of PMS/ZAMS stars. Stars in the 1st quartile (i.e. lowest mass) of the mass range of the comple sample are denoted by crosses, stars in the 2nd, 3rd, and 4th quartiles by stars, circles and lying crosses, respectively.

infrared color excess $\Delta(H - K)$ is a good measure of disk accretion and veiling. However, JW526 shows only moderate $\Delta(H - K)$ at the $3 - 4\sigma$ level above a pure stellar photosphere, thus the estimate of its luminosity presumably is not largely in error due to non-stellar contributions.

Both stars are not compatible with any model of rotational evolution, as their spin-up apparently occured much earlier than predicted. However, one possible explanation might be that for very low mass stars magnetic disk-locking fails, at least in some cases. Perhaps the stellar magnetic field never was strong enough to establish disk-locking in these stars. Note also that Carkner et al. (1996) have found unusual strong x-ray variability for XZ Tau, which perhaps could be due to 'slippage' between the field and the disk.

5.2. Rotation-activity relationship

Very closely related to the study of the evolution of rotational velocity is the investigation of stellar activity. In his pioneering work, Skumanich (1972) showed that both stellar activity and rotation decline with age on the main sequence. Observations (cf. Simon 1990, Stauffer et al. 1994) indicate that rotation is the driving parameter for activity, while age seems only important in so far as rotational velocities are a function of age. It has also been observed that stellar activity, as measured e.g. by L_X/L_{bol} or the X-ray surface flux F_{SX}, shows a saturation effect. Stellar activity increases with rotation, but at some point 'saturates' at a level that seems to depend on the area of the stellar surface. I.e. at the saturation level one observes $L_X \propto R^2$ (where R denotes the stellar radius), while F_{SX} and the ratio L_X/L_{bol} take on a constant value (cf. Fleming et al. 1989, Stauffer et al. 1994). Fig. 8 illustrates the increase of activity, as measured by L_X/L_{bol}, with decreasing rotational period, i.e. increasing angular velocity. We have coded TTSs, PTTSs, stars in α Per,
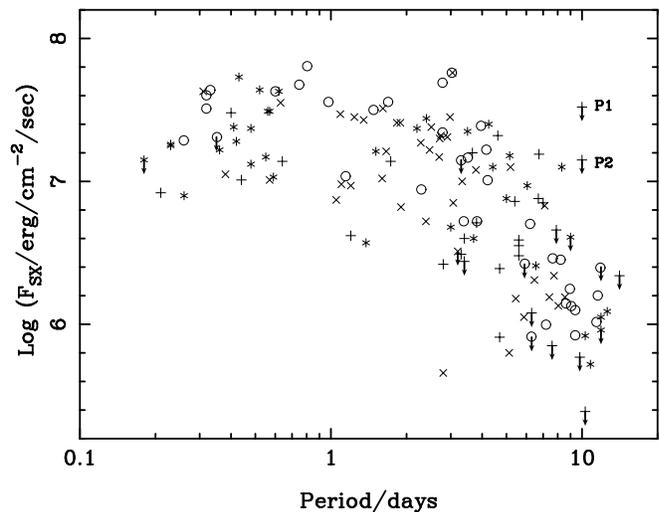
Fig. 10. X-ray surface flux $\log F_{SX}$ vs. rotational period for the quartiles of the mass distribution of the data set of PMS/ZAMS stars. Different quartiles are denoted by the same symbols as in Fig. 9

Pleiades, Hyades, by different symbols, in order to show the influence of stellar age. The observed correlation of activity and angular velocity, as well as the 'saturation' seen for the most rapid rotators, shows no trend with the age of the sample the stars pertain to. Independent of age, the samples with the most rapid rotators also contain the most active stars. Thus, indeed rotation rather than age is the driving parameter for stellar activity.

The two stars labeled by 'P1' and 'P2', which seem to lie somewhat off the general trend, are the two PTTSs RXJ1514.0-4629A and RXJ1517.8-3706A, respectively. For both of them lower limits of $P \gtrsim 10$ days have been determined. If we at-

tribute all the flux of the respective ROSAT X-ray sources to them, they are located in the plot as show. However, in both cases there is a second PTTS within the X-ray error circle, thus both have to be regarded as upper limits in L_X/L_{bol} only. RXJ1517.8-3706B has a period of 0.59 days, and, given the general trend of activity increasing with angular velocity, presumably most of the X-ray flux of this source stems from this star rather than from RXJ1517.8-3706A. RXJ1514.0-4629B showed no variability above the noise level.

In Fig. 9 we have coded the stars not by sample, but by the quartiles of the mass distribution of the whole dataset, in order to illustrate the influence of stellar mass. Apparently, stars of all masses are well mixed in the diagram, i.e. no preference of stars in some distinct mass range for some distinct location in the diagram can be seen. Therefore we conclude that rotation is much more important for stellar activity than mass. This is also apparent from Fig. 10, where we have replaced L_X/L_{bol} by the X-ray surface flux F_{SX} of the stars. Here again we see an increase of activity towards shorter periods and a saturation at the shortest periods, and again no marked dependency on the mass is visible. Note that at the very shortest periods L_X/L_{bol} as well as F_{SX} seem to decrease again. This has also been noted by Randich et al. (1996), who suggest structural changes in the star due to the very rapid rotation as a possible explanation.

In order to visualize the run of L_X/L_{bol} and F_{SX} with mass and rotational period in a more concise way, we have constructed a kind of plot known as 'control charts' (Figs. 11, 12). For these plots, we have divided our data (148 stars with L_X/L_{bol} and period known, including 14 X-ray upper limits) in ten subsets (a) by the deciles of the period distribution (in order of increasing period) and (b) by the deciles of the mass distribution (in order of increasing mass).

We then calculate the Kaplan-Meier estimator of the mean L_X/L_{bol} and F_{SX} for each subset (thus taking into account the upper limits), and plot these means vs. the number of the subset. We also draw, as horizontal lines, the mean L_X/L_{bol} or F_{SX} for the whole dataset, as well as the 95% confidence intervals for the individual subsets as derived from the Kaplan-Meier estimator.

We can see from these plots that, if divided by mass deciles, the means of the subsets do not show any significant trend with activity, and in general are found within their confidence intervals.

On the other hand, if divided by period deciles, a clear trend is apparent. The subsets with the fast rotators show high mean values of L_X/L_{bol} and F_{SX}, above the 95% confidence interval, while the subsets with the slow rotators show low mean values of L_X/L_{bol} and F_{SX}, below the 95% confidence interval. We have verified that this picture does not change qualitatively if the upper limits are skipped and the Kaplan-Meier estimator is replaced by the means of observed values. Also, as most of the stars in our sample are not originally X-ray discovered, the lack of mass dependency of activity is probably not due to X-ray selection bias.

The apparent absence of a mass-dependency indicates that the observed saturation of stellar activity for fast rotators probably is not a consequence of saturation of the internal dynamo,
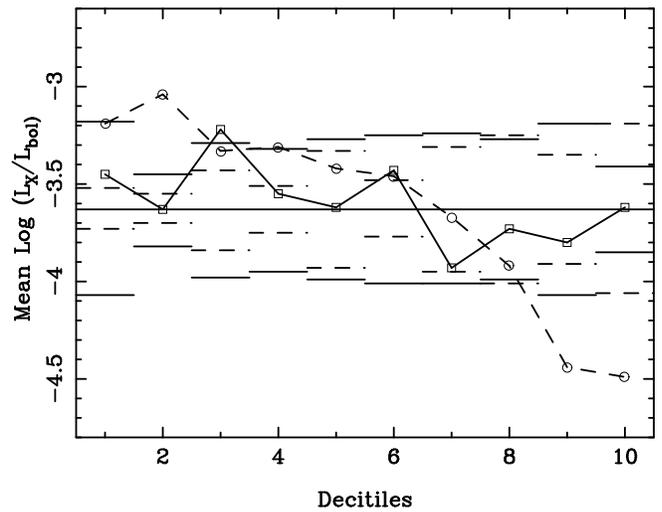

Fig. 11. Control chart for $\log(L_X/L_{bol})$. Horizontal line shows the mean (solid) for the whole dataset. Means for deciles of mass are denoted by boxes, means of deciles of period by circles. Also shown are 95% confidence intervals for the subsets (solid refers to mass deciles, dashed to period deciles).
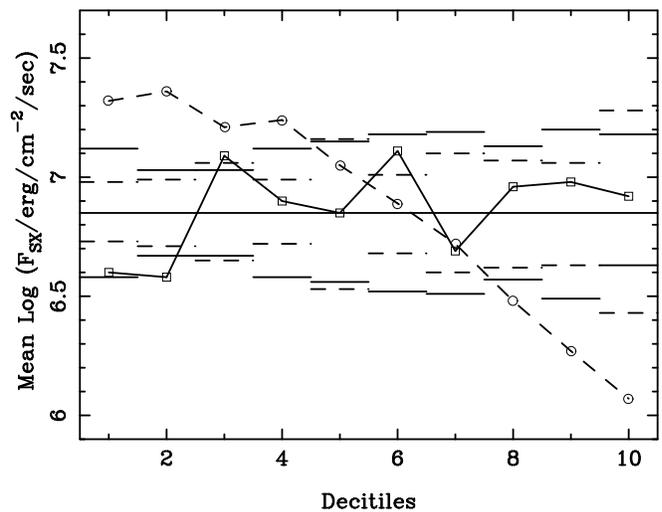

Fig. 12. Control chart for $\log F_{SX}$. For definition of symbols/lines see Fig. 11.

but rather due to some other reason, e.g. the area filling factor for magnetic flux tubes on the stellar surface. This might also be the reason for the slight trend of larger L_X/L_{bol} for smaller masses in Fig. 11 and its absence in Fig. 12. Lower mass stars have lower effective temperatures, thus the bolometric surface flux is lower and L_X/L_{bol} will increase somewhat if F_{SX} remains constant. Note however that this trend of increasing L_X/L_{bol} towards lower masses is statistically not significant with respect to tests applied to the unbinned dataset. Both the Spearman's ρ and Kendall's τ correlation coefficients yield probabilities of $P_c = 6\%$ for the hypothesis of no correlation (usual rejection limits are $P_c < 1\%$ or sometimes $P_c < 5\%$).
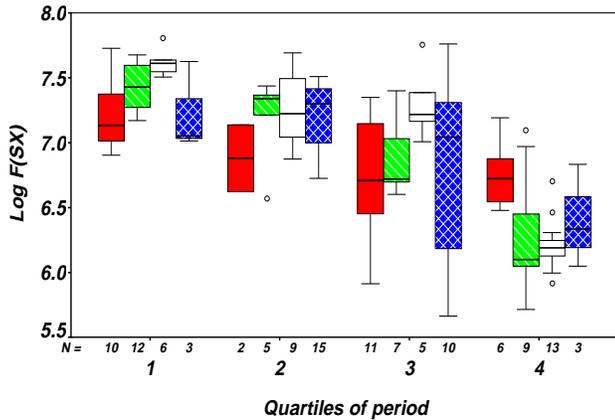
Fig. 13. Clustered boxplot of F_{SX} vs. the quartiles of the period distribution (in order of increasing period). Within each cluster, the four box-whisker symbols represent stars belonging to the 1st, 2nd, 3rd, and 4th quartile of the mass distribution (from left to right). For each period/mass quartile, the box marks the range between the upper and lower quartile (i.e. contains the central 50% of values in that group). The whiskers extend to the smallest and largest values less distant from the ends of the box than this range (i.e. less distant from the quartile points than one interquartile distance). Outliers, i.e. values more than one interquartile distance out of the quartile points, are marked by circles.

While scatterplots contain much information at the cost of visual clarity, the contrary applies to control charts. Thus, as a compromise between both, we also show a representation of the data by a clustered boxplot (Fig. 13). Here for each quartile of the period distribution four groups are formed by stars belonging to different quartiles of the mass distribution, and the median value of F_{SX} and its spread is indicated for each of the 16 groups defined in this way.

Again it appears that the saturation value for F_{SX} is rather independent of the mass of the stars. However, while for the three higher mass quartiles a sharp decline of F_{SX} for slow rotation is seen, in the lowest mass quartile the decline of F_{SX} seems to be somewhat more shallow. We have tried to verify this by statistical tests applied to the unbinned (with respect to periods) sample, but the results remain inconclusive.

The Spearman correlation test yields probabilities P_c of 0.0018, $< 10^{-4}$, $< 10^{-4}$, and 0.0007, respectively, for the four mass quartiles and the hypothesis of no correlation of F_{SX} with period. Thus, although the correlation seems somewhat worse at the lowest masses, it is still highly significant. For the slope of $\log(F_{SX})$ vs. $\log P$ we find a value of -0.56 ± 0.17 for the 1st quartile of mass, and -0.78 ± 0.12, -1.01 ± 0.13, and -0.89 ± 0.20 for the 2nd, 3rd, and 4th quartile of mass, respectively. Although the 1st quartile of mass shows the flattest slope, they all agree within $2\,\sigma$ with the mean slope (-0.81).

6. Conclusion

Based on differential CCD photometry from a single site, we could determine rotational periods for 34 out of 46 PTTSs. This clearly demonstrates that the method chosen by us is a very efficient means for determining rotational periods of spotted stars.

The results of our study indicate that the evolution of the surface angular velocity of low mass PMS/ZAMS stars depends on the stellar mass, as expected from theoretical grounds. The most prominent observed features are (i) indications of a shift of the peak of the angular velocity towards higher ages for lower masses, and (ii) high peak angular velocity are observed for stars at *all* masses within the large range of mass considered in our study. However, more data are required to improve the statistics and confirm this result.

Comparison with recent models show reasonable agreement with observations. However, at the lowest masses ($0.4-0.7M_\odot$) some uncertainties remain. Observations of a ZAMS cluster with an age of about 200 Myr would help to clarify the situation in this mass range. It would also be very interesting if more 'early spin-up' stars like XZ Tau and JW526 were found in this mass range, to see whether this phenomenon is real or rather due to large errors in the age estimates.

We also conclude that the main parameter responsible for stellar activity is the rotation. On theoretical grounds one might expect a different behavior of the dynamo for the lowest mass stars, as these stars have much deeper convection zones. However, apparently the well-known effect of 'saturation' for fast rotators shows no significant dependancy on mass, which indicates that probably it is not due to a saturation of the dynamo. There might be indications of a trend of a more shallow decrease of F_{SX} with angular velocity for the lower mass stars, but the statistical significance is low.

References

Alexander D.R., Augason G.C., Johnson H. R. 1991, ApJ 345, 1014
Allain S., Bouvier J., Prosser C.F., Marschall L.A., Laaksonen B.D. 1996a, A&A 305, 498
Allain S., Fernández M., Mart in E.L., Bouvier J. 1996b, A&A 314, 173
Allain S. et al. 1997, in: 9th Cambridge Workshop on Cool Stars, Stellar Systems and the Sun, eds. R. Pallavicini & A.K. Dupree, ASP Conf. Ser. Vol. 109, p. 353
Appenzeller I., Mundt R. 1989, A&AR 1, 291
Bessel M.S., Wood P.R. 1984, PASP 96, 247
Bouvier J. 1994, in: 8th Cambridge Workshop on Cool Stars, Stellar Systems and the Sun, ed. J.-P. Caillaut, ASP Conf. Ser. Vol. 64, p. 151
Bouvier J., Forestini M. 1994 in: Circumstellar dust disk and planetary formation, 10th IAP meeting, ed. Ferlet, p. 347
Bouvier J., Cabrit C., Fernández M., Martín E.L., Matthews J. 1993, A&A 272, 176
Bouvier J., Wichmann R., Grankin K. et al. 1997a, A&A 318, 495
Bouvier J., Forestini M., Allain S. 1997b, A&A, in press
Briceño C., Hartmann L.W., Stauffer J.R. et al. 1997, AJ 113, 740
Cameron A.C., Campbell C.G. 1993, A&A 274, 309
Cameron A.C., Jianke L. 1994, A&A 269, 1099

Cameron A.C., Campbell C.G., Quaintrell H. 1995, A&A 298, 133

Canuto V.M., Mazzitelli I. 1991, ApJ 370, 295

Carkner L., Feigelson E.D., Koyama K., Montmerle T., Reid N. 1996, ApJ 464, 286

Choi P.I., Herbst W. 1996, AJ 111, 283

Comerón F., Torra J., Gómez A.E. 1994, A&A 286, 789

D'Antona F., Mazzitelli I. 1994, ApJSS 90, 467

Dworetsky M.M. 1983, MNRAS 203, 917

Dubath P., Reipurth B., Mayor M. 1996, A&A 308, 107

Edwards S., Strom S.E., Hartigan P. et al. 1993, AJ 106, 372

Elmegreen B.G. 1985, in Protostars & Planets II, eds. D.C. Black & M.S. Matthews, Univ. of Arizona Press, Tucson, p.33

Feigelson E.D. 1996, ApJ 468, 306

Feigelson E.D., Casanova S., Montmerle T. 1993, ApJ 416, 632

Fleming, T. A., Gioia, I. M., Maccacaro, T. 1989, ApJ 340, 1011

Gahm G.F., Fischerström C., Liseau R., Lindroos K.P. 1989, A&A 211, 115

Herbig G.H. 1978, in: Problems of Physics and Evolution of the Universe, eds. L.V. Mirzoyan, Armen. Acad. of Sci., Yerevan, p.171

Horne J.H., Baliunas S.L. 1986, ApJ 302, 757

Hughes, J., Hartigan, Krautter, J., Kelemen, J. 1994, AJ 108, 1071

Jones B.F., Herbig G.H. 1979, AJ 84, 1872

Keppens R., MacGregor K.B., Charbonneau P. 1995, A&A 294, 469

Krautter J., Wichmann R., Schmitt J.H.M.M. et al. 1997, A&ASS 123, 329

Neuhäuser, R., Sterzik, M.F., Schmitt, J.H.M.M., Wichmann, R. Krautter, J. 1995, A&A 297, 391

O'Dell M.A., Panagi P., Hendry M.A., Cameron A.C. 1995, A&A 294, 715

Palla F., Galli D. 1997, ApJL 476, 35

Prosser C.F., Shetrone M.D., Dasgupta A. et al. 1995, PASP 107, 211

Pye J.P., Hodgkin S.T., Stern R.A., Stauffer J.R. 1994, MNRAS 266, 798

Radick R.R., Thompson D.T., Lockwood C.W., Duncan D.K., Bagget W.E. 1987, ApJ 321, 459

Randich S., Schmitt J.H.M.M., Prosser C.F., Stauffer J.R. 1996, A&A 305, 805

Roberts D.H., Dreher J.W. 1986, AJ 93, 968

Scargle J.D. 1982, ApJ 263, 835

Simon T. 1990, ApJL 359, L51

Simon M., Ghez A.M., Leinert Ch. 1993, ApJ 408, L33

Skumanich A. 1972, ApJ 171, 565

Soderblom D.R, Mayor M. 1993, ApJ 402, L5

Soderblom D.R., Stauffer J.R., Hudon J.D., Jones B.F. 1993, ApJS 85, 315

Stauffer J.R., Hartmann L.W., Jones B.F. 1989, ApJ 346, 160

Stauffer J.R., Caillault J.-P., Gagné M., Prosser C.F., Hartmann L.W. 1994, ApJSS 91, 625

Stern R.A., Schmitt J.H.M.M., Kahabka P.T. 1995, ApJ 448, 683

Tyson N.D., Gal R.R. 1993, AJ 105, 1206

Vrba F.R., Chugainov P.F., Bruce Weaver Wm., Stauffer J.S. 1993, AJ 106, 1608

Westin, T.N.G. 1985, A&AS 60, 99

Wichmann R., Krautter J., Schmitt J.H.M.M. et al. 1996, A&A 312, 439

Wichmann R., Krautter J., Covino E. et al. 1997a, A&A 320, 185

Wichmann R., Sterzik M., Krautter J., Metanomski A., Voges W. 1997b, A&A in press